*J. Ocean Univ. China* (Oceanic and Coastal Sea Research)
DOI 10.1007/s11802-017-3383-8
ISSN 1672-5182, 2017 16 (4): 661-673
*http://www.ouc.edu.cn/xbywb/*
*E-mail:xbywb@ouc.edu.cn*

# Violent Transient Sloshing-Wave Interaction with a Baffle in a Three-Dimensional Numerical Tank

XUE Mi-An[1), 2), 3)], ZHENG Jinhai[1), 2), *], LIN Pengzhi[4)], and XIAO Zhong[3), *]

1) *State Key Laboratory of Hydrology-Water Resources and Hydraulic Engineering*, *Hohai University*, *Nanjing* 210098, *P. R. China*
2) *College of Harbour Coastal and Offshore Engineering*, *Hohai University*, *Nanjing* 210098, *P. R. China*
3) *State Key Laboratory of Hydraulic Engineering Simulation and Safety*, *Tianjin University*, *Tianjin* 300072, *P. R. China*
4) *State Key Laboratory of Hydraulics and Mountain River Engineering*, *Sichuan University*, *Chengdu* 610065, *P. R. China*

(Received January 3, 2017; revised May 11, 2017; accepted May 17, 2017)


**Abstract** A finite difference model for solving Navier Stokes equations with turbulence taken into account is used to investigate viscous liquid sloshing-wave interaction with baffles in a tank. The volume-of-fluid and virtual boundary force methods are employed to simulate free surface flow interaction with structures. A liquid sloshing experimental apparatus was established to evaluate the accuracy of the proposed model, as well as to study nonlinear sloshing in a prismatic tank with the baffles. Damping effects of sloshing in a rectangular tank with bottom-mounted vertical baffles and vertical baffles touching the free surface are studied numerically and experimentally. Good agreement is obtained between the present numerical results and experimental data. The numerical results match well with the current experimental data for strong nonlinear sloshing with large free surface slopes. The reduction in sloshing-wave elevation and impact pressure induced by the bottom-mounted vertical baffle and the vertical baffle touching the free surface is estimated by varying the external excitation frequency and the location and height of the vertical baffle under horizontal excitation.

**Key words** transient sloshing wave; vertical baffle; excitation frequency; experimental and numerical study

## 1 Introduction

Liquid sloshing is a strongly nonlinear fluid motion with a free surface and is highly relevant in the design of partially filled containers with fluids. Liquid sloshing has becomes increasingly important in the fields of naval architecture and ocean engineering given the increasing sizes of fluid-containing tanks. Interest has been growing with regard to the development of new large marine vehicles for transportation of liquid natural gas (LNG) and liquid petroleum gas (LPG). However, highly localized impact pressure caused by violent sloshing fluid could damage the walls of the tank and produce sufficiently large moments to destabilize the vehicle that carries partially fluid-filled containers, especially when the forcing frequency is close to the natural frequency of the liquid-tank itself. To minimize the potential sloshing damage, the control of the sloshing behavior with baffles has been a subject of interest in recent years. The vertical baffle is a sharp edged baffle that is considered a more effective anti-sloshing means under horizontal excitation. It is also commonly know that a typical baffle configuration for current LPG tanks consists of a stack of vertical or horizontal baffles fitted around the inner periphery of the tank. How does the vertical baffle dampen the sloshing and its effectiveness is still a hot research topic. Buzhinskii (1998) considered that the formation of vortices occurs at these sharp edges, and the vortex motion of the fluid is localized in small neighborhoods of the sharp edges of the vertical baffles. The baffle-induced fluid sloshing attenuation is associated with the transfer of energy from an irrotational form of motion to a vortex form of motion due to energy dissipation in small-scale vortices. Tuner *et al*. (2013) considered that the sloshing attenuation can be accomplished first and foremost by simply blocking the fluid motion. A second more subtle effect of the baffles is to change the natural frequency of the fluid. Similar conclusions have ever been summarized in reference (Xue and Lin, 2011). Because of the complexity of sloshing, studies and analyses on the sloshing dynamics are significant for designing LNG/LPG or other liquid storage tanks.

Many numerical investigations of liquid sloshing in a tank with the baffles have been conducted in the past years. Rebouillat and Liksonov (2010) discussed the sloshing problems and corresponding numerical approaches used to predict sloshing-wave amplitude, frequency, pressure and the effects of sloshing on stability in the container environment. About the study of the baffles

* Corresponding authors. E-mail: jhzheng@hhu.edu.cn
E-mail: tjuzhongxiao@tju.edu.cn

in reducing sloshing, Gedikli and Erguven (1999) concluded that the decreases in the ratio of overturning moments is strictly larger than the increases in the ratio of shear force by installing a rigid baffle into a cylindrical tank under the seismic excitation. Cho *et al.* (2002) examined the parametric ring baffle effects on the natural frequency of freely vibrated baffled tanks. In fact, the forced sloshing problem is more important in practical engineering. Kim and Lee (2008) mainly focused on optimizing the length and width of the horizontal baffles to reduce sloshing effects by applying the evolutionary optimization method. The baffle damping mechanism is thus not referred in their studies. Liu and Lin (2009) studied three-dimensional sloshing in a tank with a horizontal baffle and a vertical baffle, and concluded that the vertical baffle is more effective in reducing the sloshing amplitude. For the problem, Shin *et al*. (2005) confirmed that vertical baffles are effective for shallow filling-depth application and horizontal baffles are useful for non-shallow filling-depth. Further, Akyildiz (2012) investigated the effects of bottom-mounted vertical baffle height on liquid sloshing in a rolling rectangular tank, and concluded that the rolling motion of the liquid and the vortex originated by the flow separation from the baffle tip becomes weaker with increasing the baffle height. He considered that the blockage effect of the baffle on the liquid convection is predominant. Meanwhile, the inertial forces were not enough to propel the liquid to reach to the top wall of the tank. Qin *et al*. (2013) conducted a study of sloshing in a tank with horizontal baffles and found that the viscous fluid model can more predict reasonably the physical dissipation than the potential flow models, especially the strong flow shear and significant vortex shedding in the flow field due to the existence of the baffles. Lu *et al*. (2015) concluded that the dissipative effects have significant influence on the sloshing responses in both non-baffled and baffled tanks. Especially the sloshing in baffled tank involves more dissipation due to the stronger vortices flow, which is one of the main damping mechanisms of the baffles.

Experimental approaches are the most reliable methods of estimating actual dynamic characteristics of sloshing with the improvement of experimental devices. Many researchers have conducted experimental studies on liquid sloshing to estimate the pressure distribution on the tank walls and the free surface elevation variation with the time series. Younes *et al*. (2007) investigated experimentally the effects of the upper, lower, and holed vertical baffles on system damping in a freely vibrated tank. Results showed that the size and location of the vertical baffles influence hydrodynamic damping significantly. However, because only the free vibration test can be conducted in their study, the relation between sloshing response amplitude and forcing frequency is not investigated. Gandhi *et al*. (2008) developed a new 2 DOF actuation slosh rig to study liquid sloshing phenomenon in a tank that is usually subjected to forced lateral and pitching motions. The effect of the baffles in reducing sloshing is not discussed temporarily in the study. As pioneers in this fields, Ibrahim (2005) and Faltinsen and Timokha (2009) presented an extensive review of previous theoretical and experimental research on sloshing in tanks with and without baffle. However, it can be found that the effect of the vertical baffle touching the free surface in reducing sloshing is seldom studied parametrically.

In this study, an in-house numerical model (Liu and Lin, 2008; Xue and Lin, 2011) and a liquid sloshing experimental apparatus (Xue *et al*., 2013, 2017) are employed to further estimate effects of two types of vertical baffle on attenuating sloshing in a prismatic tank by varying the location and height of the vertical baffle and the forcing frequency. The numerical results are validated against the present experimental data for strongly nonlinear sloshing in a tank without and with the vertical baffle, respectively. Fast Fourier transform analyses are used to conduct a spectral analysis of the time histories of the free surface elevation and identify the dominant response frequencies of sloshing in a rectangular tank with the vertical baffle.

## 2 Mathematical Model

The air phase is computed simultaneously with water phase as two incompressible, viscous fluids. The motions of the air and water phases are governed by the Navier Stokes and continuity equations

$$\frac{\partial u_j}{\partial x_j} = 0 , \tag{1}$$

$$\frac{\partial u_i}{\partial t} + u_j \frac{\partial u_i}{\partial x_j} = -\frac{1}{\rho}\frac{\partial p}{\partial x_i} + f_i + \nu_{eff} \frac{\partial^2 u_i}{\partial x_j \partial x_j} , \tag{2}$$

where $i$ represents the degree of freedom; $I=1,2,3$ indicates three components in the $x$, $y$, and $z$ directions; $j$ denotes the summation symbol; $u_i$ stands for the velocity component in the $x_i$ direction; and $\rho$, $p$, $\nu_{eff}$, and $f_i$ are the fluid density, pressure, effective kinematic eddy viscosity and $i$-th component of the external force accelerations (including the gravitational acceleration), respectively.

The improved free-slip boundary condition is imposed on the solid walls, *i.e*., $u_n = 0$, $\partial u_t/\partial \boldsymbol{n}=0$ and $\partial p/\partial \boldsymbol{n}=0$, where $\boldsymbol{n}$ is the unit vector normal to the boundary and pointing out of the fluid, $u_n$ and $u_t$ is respectively the normal velocity and tangential velocity component near the solid wall. In the two-phase flow model, air and water are computed simultaneously in the physical computational domain. The free surface boundary condition is thus no need to be considered here. In non-inertial coordinate system, the velocity of the fluid particle relative to the moving tank is $\boldsymbol{u}$, and the velocity of the moving tank relative to the earth ground is $\boldsymbol{U}_0$. At $t=0$, if the fluid inside the tank starts to move from the static state, the velocity of the fluid particle relative to the earth ground should be $\boldsymbol{U}=\boldsymbol{u}+\boldsymbol{U}_0=0$, *i.e*., $\boldsymbol{u}=-\boldsymbol{U}_0$. In numerical simulation, the static fluid pressure is used as the initial pressure field.

In this model, the large-eddy simulation technique is

used to model turbulence by using the Smagorinsky subgrid scale model. The second-order accurate volume-of-fluid method is used to track the possible broken free surface. The virtual boundary force method is employed to model the internal baffles inside the tanks. Detailed illustrations of the numerical model can be found in our previous paper (Xue and Lin, 2011).

## 3 Experimental Setup

In this study, a shaker table driven by a wavemaker for the liquid sloshing experiment is developed to study the nonlinear behaviors of liquid sloshing and the baffle damping characteristics in a rectangular tank. The experimental apparatus consists of a wavemaker, a liquid tank, a displacement sensor, wave gauges, pressure sensors and a computer. A schematic of the experimental apparatus is shown in Fig.1. The wavemaker is a wave generator driven by an electro-hydraulic servo system, related computer control, data acquisition and analysis system. It can generate regular motion such as cosine function. A rectangular tank is secured on a shaker table that can be moved back and forth and precisely controlled by a wavemaker. During the experiments, a displacement sensor is used to record the time history of the motion of the tank, and three wave gauges are fixed separately on the tank to record the temporal evolution of the free surface elevation. Each wave gauge sensor is a capacitance probe that detects the change in water level precisely with no time lag. The wave gauge sensors are used in conjunction with a signal-processing unit in which the capacitance values were transformed to a voltage signal, and they can simultaneously record the sloshing-wave elevation near the periphery of the tank wall from predetermined locations to provide the free surface profiles of liquid at the desired time interval. The pressure sensor with the sampling frequency of 1000 Hz is used in this study for exactly seizing the impulse pressure.

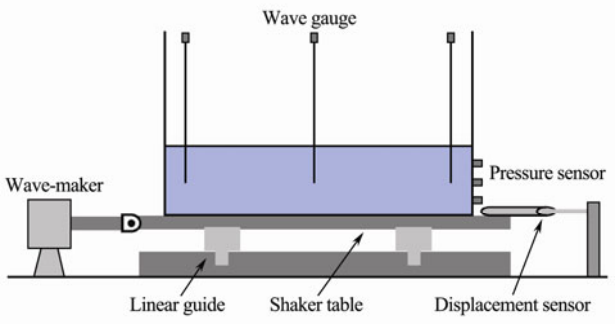


Fig.1 Experimental setup of the liquid sloshing.

## 4 Results and Discussion

### 4.1 Liquid Sloshing with a Bottom-Mounted Vertical Baffle

In this section, the experimental data are presented to assess the accuracy of the three-dimensional numerical results of sloshing in a rectangular prism tank with a bottom-mounted vertical baffle. A schematic illustration of sloshing in a rectangular prism tank with a bottom-mounted vertical baffle is shown in Fig.2. In the experiments, three wave gauges and three pressure sensors are mounted on the rectangular prism tank to record the time series of the free surface elevation and pressure acting on the tank wall. The following are the dimensions of the rectangular tank: $L=0.57$ m, $W=0.31$ m, and $H=0.7$ m. A vertical baffle that is 0.31 m wide, 0.15 m high, and 0.006 m thick is installed inside the rectangular prism tank, which is at a distance of $d=0.275$ m from the left boundary of the tank. The height of the vertical baffle is denoted by $h_b$. The rectangular prism tank partially filled with water at a depth of $h=0.2$ m is fixed on a shaker table and subjected to a cosine function $x=-a\cos\omega t$, where $a=0.03$ m is the amplitude of the tank movement. The corresponding lowest natural frequency $\omega_0=6.5823\,\mathrm{rad\,s^{-1}}$ is calculated according to the following dispersion equation

$$\omega_n=\sqrt{(g(2n+1)\pi/L)\tanh(h(2n+1)\pi/L)},\ n=0,1,2,\cdots, \tag{3}$$

where $\omega_n$ and $n$ is the angular frequency and the mode number. The external excitation frequency is $\omega=\omega_0$. The parameters are summarized as in Table 1.

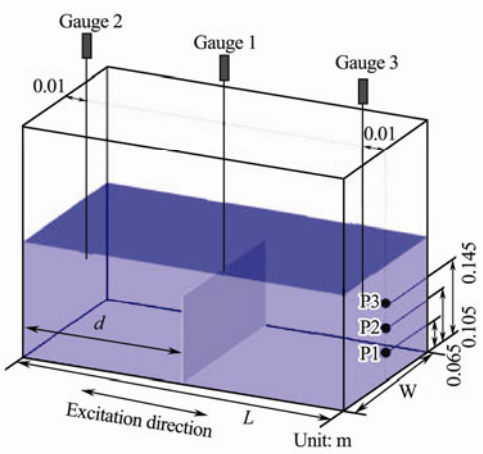


Fig.2 Liquid sloshing in a rectangular tank with a bottom-mounted vertical baffle.

Numerical simulation is conducted according to the above experiment. According to the mesh convergence test of Fig.2 conducted by Liu and Lin (2008), the mesh system with $57\times31$ uniform meshes with the mesh size $\Delta x=\Delta y=0.01$ m in the horizontal plane and 80 uniform meshes with the mesh size $\Delta z=0.005$ m in the vertical direction are employed here to discretize the three-dimensional computational domain of $0.57\,\mathrm{m}\times0.31\,\mathrm{m}\times0.4$ m. The time step would be self-adjusted according to the stability criteria. The turbulent model is turned on in this simulation. The origin of the coordinate system is the center of the tank and on the static free surface. Water with a density of $\rho_l=1000\,\mathrm{kg\,m^{-3}}$ and kinematic viscosity of $v_l=1.14\times10^{-6}\,\mathrm{m^2\,s^{-1}}$ and air with a density of $\rho_g=1\,\mathrm{kg\,m^{-3}}$ and kinematic viscosity of $v_g=1.5\times10^{-5}\,\mathrm{m^2\,s^{-1}}$ are adopted in this simulation. Fig.3 shows comparisons of

the time histories of the free surface elevation at wave gauges 1, 2, and 3 and the pressure at sensors P1, P2, and P3 between the numerical results and the experimental data for sloshing in the tank with the bottom-mounted vertical baffle when the excitation frequency is $\omega=\omega_0=6.5823\,\mathrm{rad\,s^{-1}}$. Fig.3 shows that the numerical results are in good agreement with the experimental data of both free surface and pressure for three-dimensional liquid sloshing in a rectangular prism tank with the bottom-mounted vertical baffle.

Table 1 Parameters used in the sloshing with a bottom-mounted vertical baffle

| Parameters | Value |
|---|---|
| Tank size: $L \times W \times H$ | 0.57 m × 0.31 m × 0.4 m |
| Vertical baffle size: height × width × thickness | 0.15 m × 0.31 m × 0.006 m |
| Water depth: $h$ | 0.2 m |
| Movement equation of the tank | $x=-a\cos\omega t$ |
| Amplitude: $a$ | 0.03 m |
| Frequency: $\omega$ | $6.5823\,\mathrm{rad\,s^{-1}}$ |
| Distance of the vertical baffle from the tank left wall: $d$ | 0.275 m |

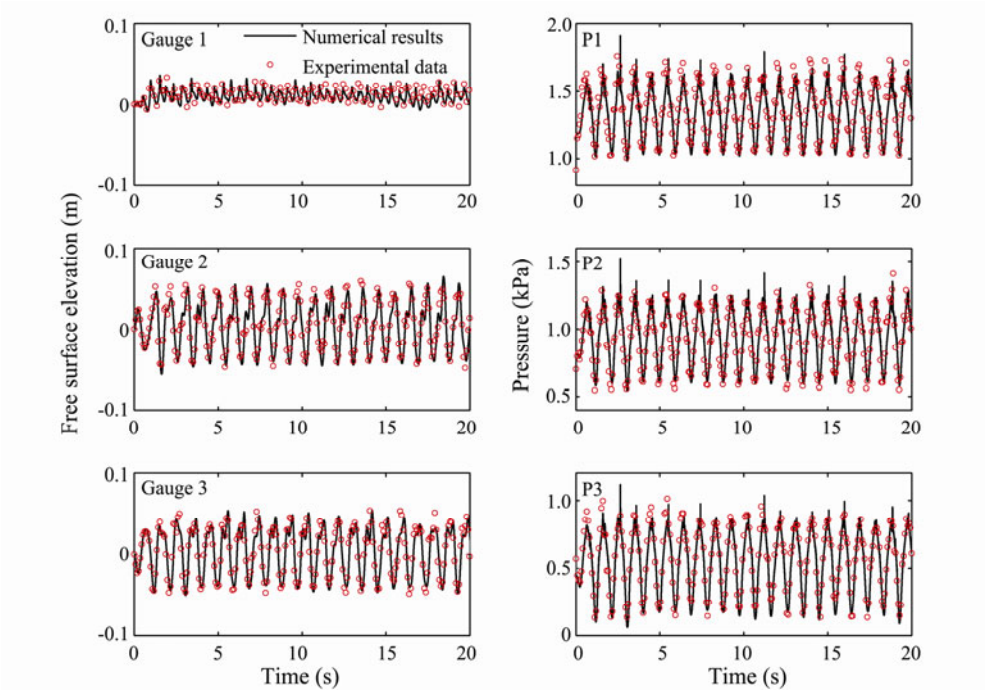


Fig.3 Comparisons of the time histories of the free surface elevation at wave gauges 1, 2, and 3 and the pressure at sensors P1, P2, and P3 between the numerical results and the experimental data for sloshing in the tank with a bottom-mounted vertical baffle, when $x=-a\cos\omega t$, $a=0.03$ m, $h=0.2$ m, $\omega=\omega_0$, $d=0.275$ m and $h_b=0.15$ m.

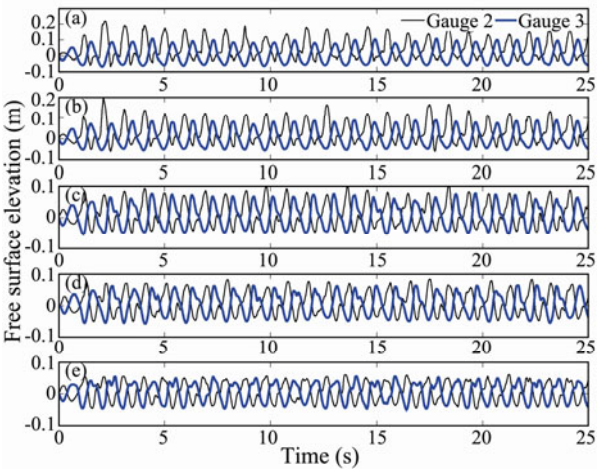


Fig.4 Comparisons of the time histories of the free surface elevation at wave gauges 2 and 3 for the different values of the parameter $d$: (a) $d=0.175$ m, (b) $d=0.2$ m, (c) $d=0.234$ m, (d) $d=0.25$ m, (e) $d=0.275$ m.

Effects of the bottom-mounted vertical baffle location on the free surface elevation are studied by varying the distance $d$ of the vertical baffle to the left tank wall. The other parameters are the same except parameter $d$. Fig.4 shows comparisons of the time histories of the free surface elevation at wave gauges 2 and 3 for the different values of the parameter $d$. Fig.4 shows that the free surface elevation at wave gauges 2 and 3 will decrease to a minimum value with the increasing distance of $d$ to the left tank wall until the vertical baffle is in the center of the tank, thereby indicating that the vertical baffle located at the center of the tank can maximally reduce the sloshing amplitude. Moreover, Fig.4(a–d) shows that the free surface elevation at wave gauge 2 is slightly larger than that at wave gauge 3 because of the asymmetrical location of vertical baffle installed inside the tank.

Fig.5 plots the amplitude spectrum of the free surface elevation at wave gauges 2 and 3 for the different values

of the parameter $d$. The main peak frequencies of 1.0498 and 2.0996 are given in Fig.5. The excitation frequency $f=\omega/2\pi=1.0476$ Hz is just about equal to the first peak frequency. The energy of the sloshing wave excited by the external forces is mainly distributed in the excitation frequency and its double frequency, and it decreases gradually when the bottom-mounted vertical baffle is moved to the center of the tank.

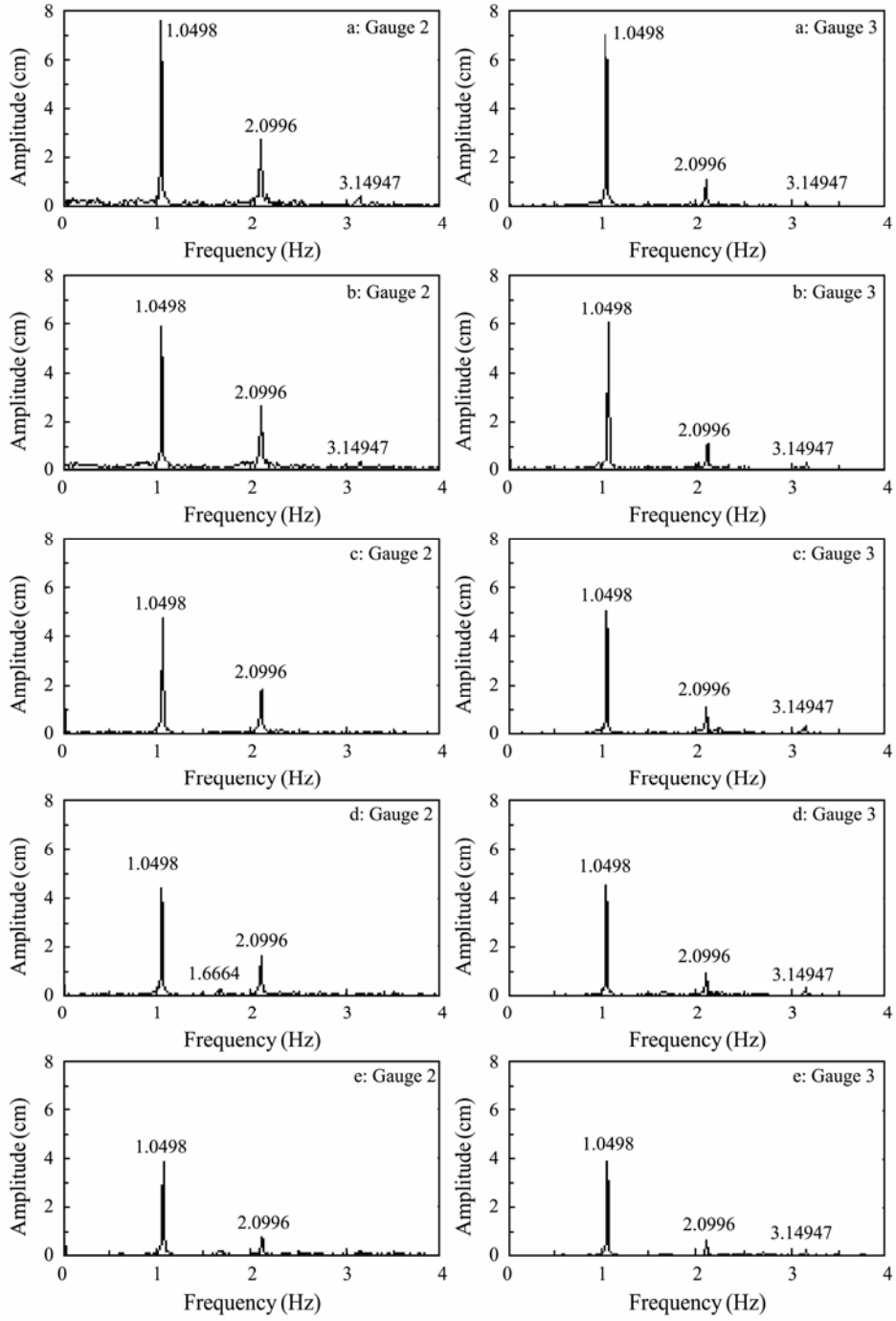


Fig.5 Amplitude spectrum of the free surface elevation at wave gauges 2 and 3 for the different values of parameter $d$: (a) $d=0.175$ m, (b) $d=0.2$ m, (c) $d=0.234$ m, (d) $d=0.25$ m, (e) $d=0.275$ m.

Effects of the bottom-mounted vertical baffle height on the free surface elevation are studied numerically. The other parameters are the same except the bottom-mounted vertical baffle height. The water depth is $h=0.2$ m. Therefore, the bottom-mounted vertical baffle is divided into three types, namely, immersed baffle, baffle flushing with free surface, and surface-piercing baffle according to the ratio of the vertical baffle height to water depth. Fig.6 shows comparisons of the time histories of the free surface elevation at wave gauges 2 and 3 for the bottom-mounted vertical baffle with different $h_b$: (a) $h_b=0.00$ m, (b) $h_b=0.15$ m, (c) $h_b=0.20$ m, (d) $h_b=0.25$ m when the bottom-mounted vertical baffle is located at a distance of $d=0.275$ m to the left tank wall. The bottom-mounted vertical baffles effectively reduce the free surface elevation. The wave amplitude attenuation caused by the ver-

tical baffle can be simply defined as

$$Dr = (\eta^1_{\max} - \eta^2_{\max})/\eta^1_{\max} \times 100\% , \quad (4)$$

where $\eta^1_{\max}$ is the maximum free surface elevation of sloshing in a tank without baffle, $\eta^2_{\max}$ is the maximum free surface elevation of sloshing in a tank with the vertical baffle, and $Dr$ is the wave amplitude attenuation of the maximum free surface elevation. The wave amplitude attenuations of 85.0%, 81.5%, and 84.9% are estimated for the immersed baffle, the baffle flushing with free surface, and the surface-piercing baffle, respectively. The immersed baffle is therefore considered a better anti-sloshing baffle than the others. However, Fig.6(d) shows that the sloshing amplitude is less than that in Fig.6(b) when the time history of the free surface elevation reaches a steady state.

Fig.7 shows the amplitude spectrum of the free surface elevation at wave gauge 2 for the different $h_b$: (a) $h_b$= 0.00 m, (b) $h_b$=0.15 m, (c) $h_b$=0.20 m, (d) $h_b$=0.25 m, respectively. All the dominant peak frequencies are near the external excitation frequency, and the low frequencies before the dominant peak frequency are filtered out when a vertical baffle is installed inside the tank. Moreover, sloshing-wave kinetic energy decreases with an increase in the height of the vertical baffle.

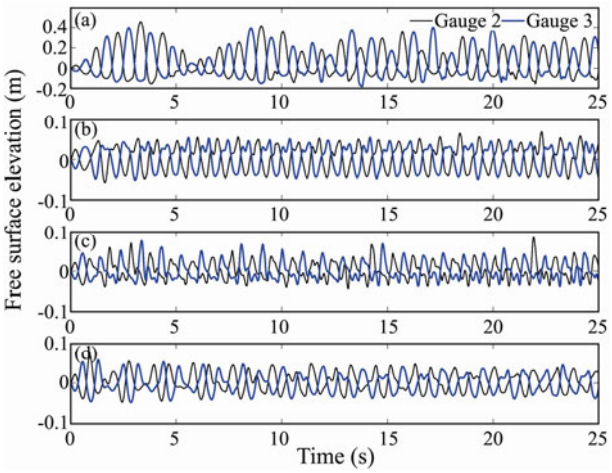


Fig.6 Comparisons of the time histories of the free surface elevation at wave gauges 2 and 3 for the bottom-mounted vertical baffle with $d$=0.275 m and different $h_b$: (a) $h_b$= 0.00 m, (b) $h_b$=0.15 m, (c) $h_b$=0.20 m, (d) $h_b$=0.25 m.

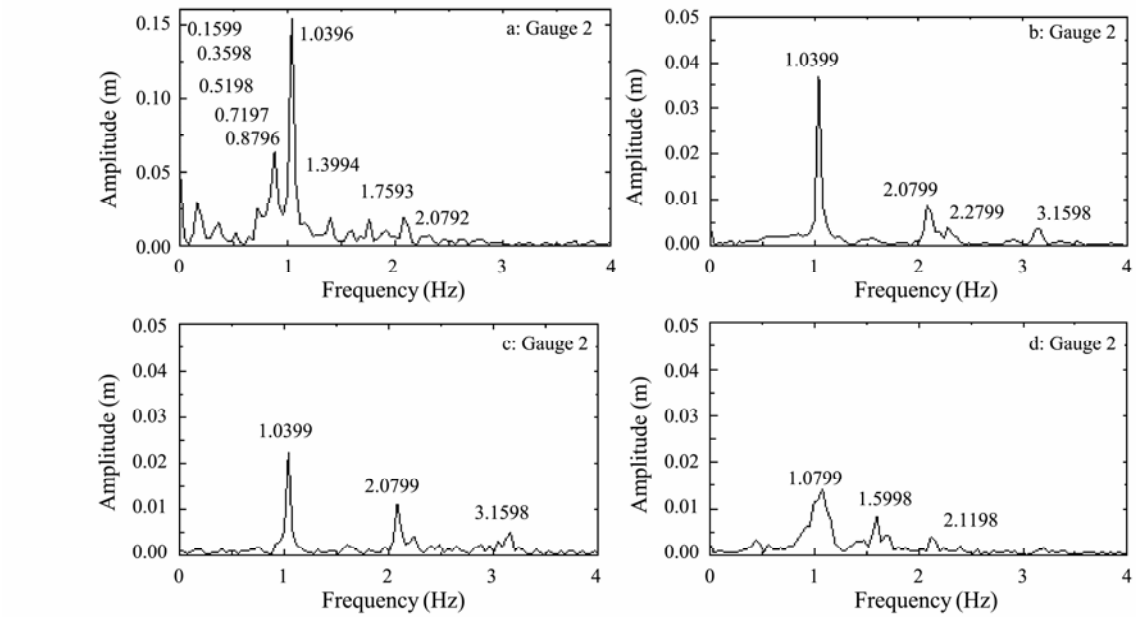


Fig.7 Amplitude spectrum of the free surface elevation at wave gauge 2 for the different $h_b$: (a) $h_b$=0.00 m, (b) $h_b$=0.15 m, (c) $h_b$=0.20 m, (d) $h_b$=0.25 m.

Effects of the excitation frequency on the free surface elevation are studied numerically and experimentally. The maximum free surface elevation at a fixed probe is generally considered the maximum value before wave breaking. In this study, the maximum free surface elevation is extended to a maximum value during sloshing periods since the initial moment. The maximum free surface elevation at wave gauges 2 and 3 as a function of the excitation frequency with $h_b$=0.15 m, $x = -a\cos\omega t$, $a$=0.03 m, $h_b$ =0.2 m, $\omega_0$=6.5823 rad s$^{-1}$, and $d$=0.275 m is plotted in Fig.8. The first-mode natural frequency of the baffled tank is approximately $0.77\omega_0$, which is shifted to a lower frequency compared with the first natural frequency of the un-baffled tank. Moreover, the sloshing response amplitude excited by the second-mode frequency is much larger than that excited by the first-mode frequency. In addition, the numerical results are in fairly good agreement with the experimental data. The wave gauge in experiments records the free surface elevation variation after considering air entrainment. The value of the numerical wave gauge is obtained by integrating the fluid volumetric fraction in the vertical direction. The experimental data are therefore slightly larger than the numerical results around the first natural frequency due to breaking

waves and numerous air bubbles in the liquid.

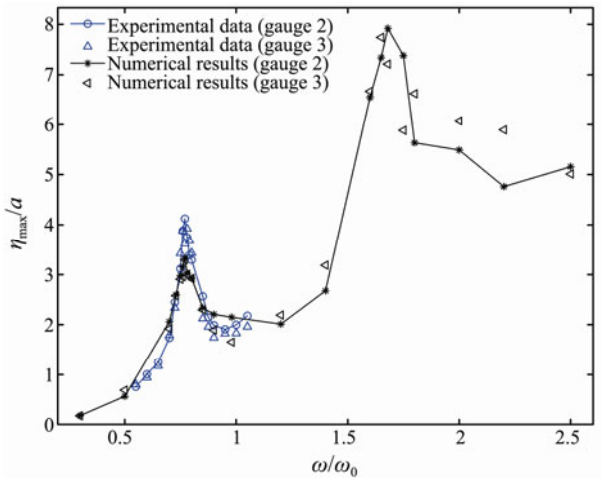


Fig.8 Maximum free surface elevation at wave gauges 2 and 3 as a function of the excitation frequency with $h_b$= 0.15 m, $x=-a\cos\omega t$, $a$=0.03 m, $h$=0.2 m, $\omega_0$=6.5823 rad s$^{-1}$, $d$=0.275 m.

The resonant sloshing in a baffled rectangular tank is considered to check the effects of the bottom-mounted vertical baffle on the free surface elevation and pressure on the tank walls. Fig.9 shows comparisons of the time histories of the free surface elevation at wave gauges 1, 2, and 3 and the pressure at sensors P1, P2, and P3 between the numerical results and the experimental data of sloshing in a tank with a bottom-mounted vertical baffle of $h_b$= 0.15 m when $x=-a\cos\omega t$, amplitude $a$=0.03 m, water depth $h$=0.2 m, frequency $\omega$=0.77$\omega_0$, and the distance to the left tank wall $d$=0.275 m. The numerical results of the free surface elevation at wave gauges 1, 2, and 3, especially for the pressure at sensors P1, P2, and P3, match well with the experimental data, thereby indicating that the present model can reasonably predict pressure distribution after considering air entrainment and wave breaking. Furthermore, the bottom-mounted vertical baffle can enhance the fluid motion through resonance aside from its blocking effects. This finding is consistent with the results of Turner *et al.* (2013).

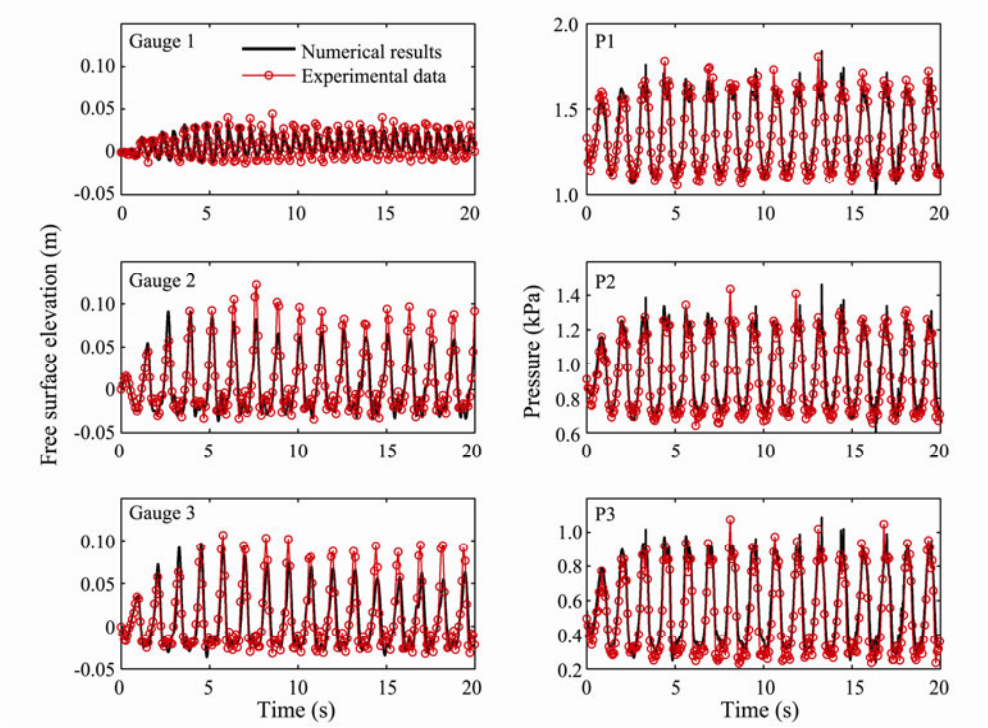


Fig.9 Comparisons of the time histories of the free surface elevation at wave gauges 1, 2, and 3 and the pressure at sensors P1, P2, and P3 between the numerical results and the experimental data when $h_b$=0.15 m, $x=-a\cos\omega t$, $a$=0.03 m, $h$= 0.2 m, $\omega$=0.77$\omega_0$, $d$=0.275 m.

Fig.10 plots the time history of the free surface elevation at wave gauge 2 and the corresponding power spectrum for sloshing in a tank (a) without baffle and frequency $\omega=\omega_0$, (b) with 0.15 m high vertical baffle and $\omega=\omega_0$, and $d$=0.275 m, (c) with a 0.15 m high vertical baffle and $\omega$ = 0.77$\omega_0$, and $d$ = 0.275 m, respectively. Figs.10(a, b, A, and B) shows that the vertical baffle not only reduces the sloshing amplitude and energy but also changes the energy distribution in frequency. The dominant frequency obtained from Figs.10(A and B) is 1.05 Hz, which is approximately equal to the excitation frequency of 1.047 Hz. The dominant frequency of 0.7998 Hz is also approximately equal to the excitation frequency of 0.8066 Hz in Fig.10(C). Figs.10(b, c, B, and C) shows that the sloshing amplitude increases, and the energy changes from a higher frequency to a lower frequency when the excitation frequency $\omega=\omega_0$ is changed into $\omega$=0.77$\omega_0$, thereby indicating that the natural frequency is shifted to a lower frequency compared with the sloshing in a tank without baffle.

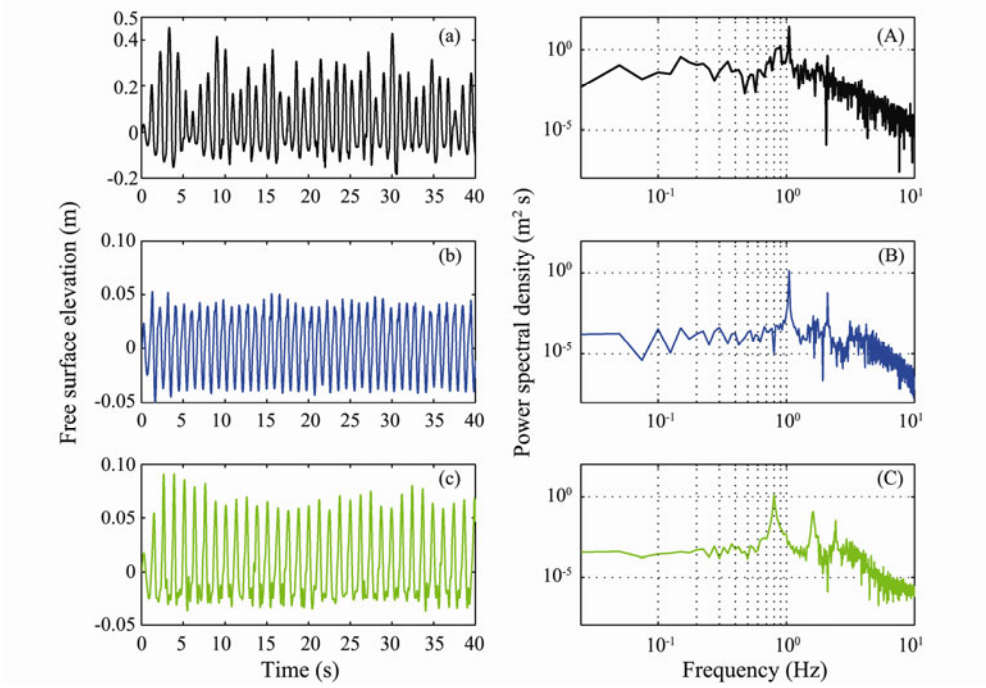


Fig.10 Time history of the free surface elevation at wave gauge 2 and the corresponding power spectrum: (a) without baffle and $\omega=\omega_0$, (b) 0.15 m high vertical baffle and $\omega=\omega_0$, and $d=0.275$ m, (c) 0.15 m high vertical baffle and $\omega=0.77\omega_0$, and $d=0.275$ m.

### 4.2 Liquid Sloshing with a Vertical Baffle Touching the Free Surface

In this section, experimental data are presented to assess the accuracy of the numerical results of sloshing in a rectangular prism tank with a vertical baffle touching the free surface. A schematic illustration of the position of the vertical baffle inside the rectangular prism tank is shown in Fig.11. The height of the vertical baffle touching the free surface is still denoted by $h_b$. Its top has a height equal to the water depth, and its bottom has a distance of $b=0.05$ m from the tank bottom. The other parameters employed here, such as tank size, vertical baffle size, water depth, movement equation, excitation amplitude and frequency, distance of the vertical baffle from the left boundary of the tank, and locations of the three wave gauges and pressure sensors, are the same as in Table 1.

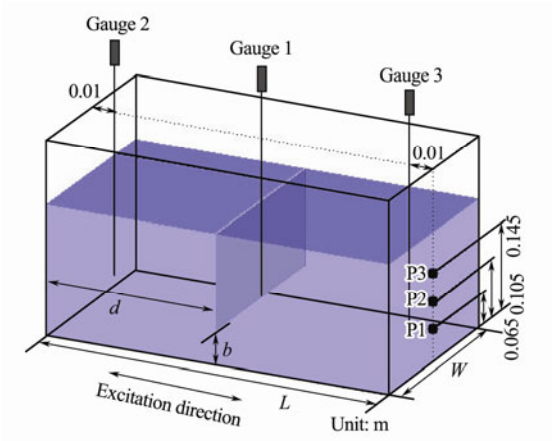


Fig.11 Liquid sloshing in a rectangular tank with a vertical baffle touching the free surface.

In the simulation, the mesh system with $57\times31$ uniform meshes with a mesh size $\Delta x=\Delta y=0.01$ m in the horizontal plane and 64 uniform meshes with a mesh size $\Delta z=0.005$ m in the vertical direction are employed to discretize the three-dimensional computational domain of 0.57 m × 0.31 m × 0.32 m. The time step would be self-adjusted according to the stability criteria. The turbulent model is turned on, and the origin of the coordinate system is the center of the tank and on the static free surface.

Fig.12 shows comparisons of the time histories of the free surface elevation at wave gauges 1, 2, and 3 and pressure at sensors P1, P2, and P3 between the numerical results and the experimental data for sloshing in the tank with a vertical baffle touching the free surface when $x=-a\cos\omega t$, $a=0.03$ m, $h=0.2$ m, $\omega=\omega_0$, $d=0.275$ m and $h_b=0.15$ m. Fairly good agreement in free surface and pressure is found between the numerical results and the experimental data for sloshing in a rectangular tank with the vertical baffle touching the free surface. Thus, the proposed numerical model can predict complex characteristics of the sloshing problem interaction with the vertical baffle touching the free surface.

Effects of the location of the vertical baffle touching the free surface on the free surface elevation are studied by varying the distance $d$ of the vertical baffle to the left tank wall. The other parameters are the same except parameter $d$. Fig.13 shows comparisons of the time histories of the free surface elevation at wave gauges 2 and 3 for the different values of the parameter $d$ for sloshing in a rectangular tank with the vertical baffle touching the free surface. Fig.13 shows that the damping effect of the vertical baffle touching the free surface is most remarkable when it is only located at the center of the tank.

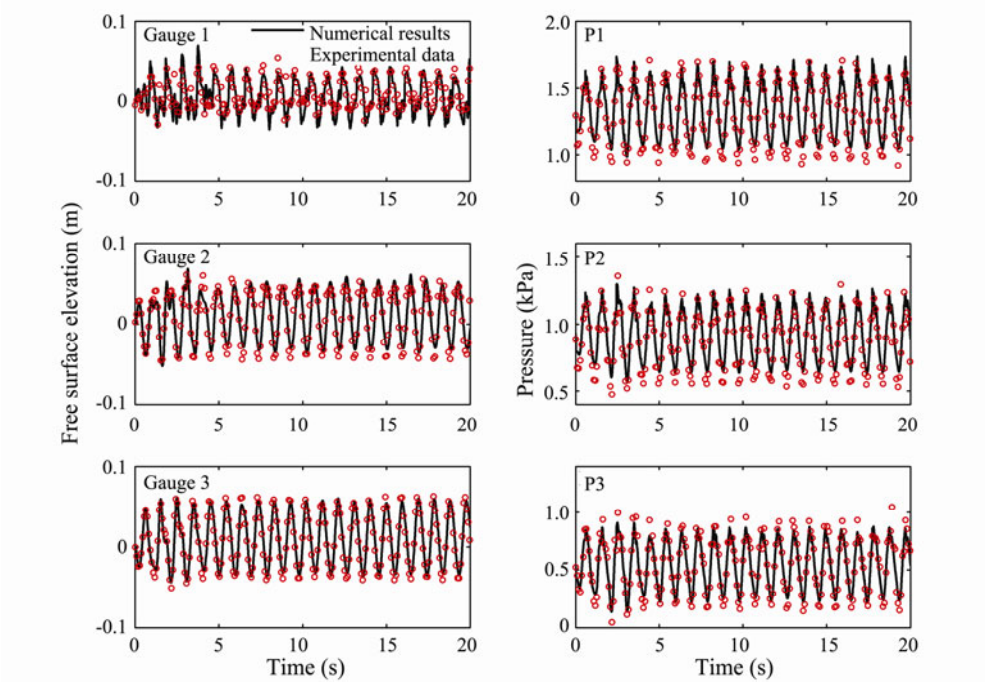


Fig.12 Comparisons of the time histories of the free surface elevation at three wave gauges 1, 2, and 3 and the pressure at sensors P1, P2, and P3 between the numerical results and the experimental data for sloshing in the tank with a vertical baffle touching the free surface when $x=-a\cos\omega t$, $a=0.03$ m, $h=0.2$ m, $\omega=\omega_0$, $d=0.275$ m, $h_b=0.15$ m.

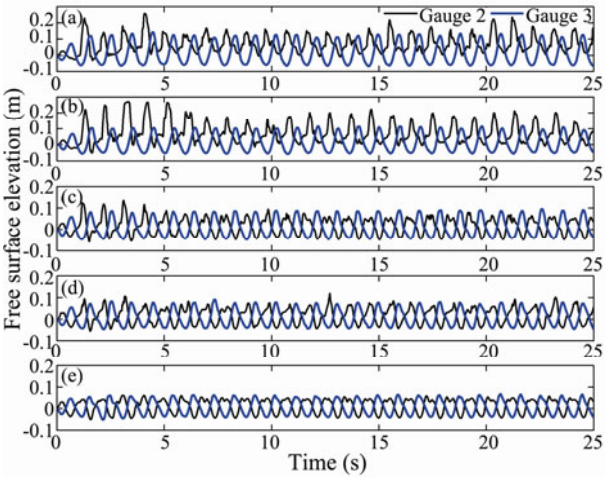


Fig.13 Comparisons of the time histories of the free surface elevation at wave gauges 2 and 3 for the different values of the parameter $d$: (a) $d=0.175$ m, (b) $d=0.2$ m, (c) $d=0.234$ m, (d) $d=0.25$ m, (e) $d=0.275$ m.

Fig.14 shows the maximum free surface elevation at wave gauges 2 and 3 in the first 25 s response to the distance of the vertical baffle from the left boundary of the tank for sloshing in a rectangular prism tank with a bottom-mounted vertical baffle and the vertical baffle touching the free surface, respectively. Fig.14 shows that the maximum free surface elevation at wave gauges 2 and 3 decreases with increasing $d$ until the vertical baffle is located at the center of the tank. This because that the maximum horizontal velocity component appears generally at the center of tank. The effectiveness of the vertical baffle in blocking horizontal velocity can thus play the biggest effect. In addition, for sloshing with the vertical baffle touching the free surface, the maximum free surface elevation at wave gauges 2 and 3 is larger than that of sloshing with the bottom-mounted vertical baffle, thereby indicating that when the vertical baffle is not at the center of the tank, its ability to reduce the maximum sloshing amplitude is reduced when it is moved to the free surface from the bottom of the tank. Figs.13 and 14 show that the vertical baffle touching the free surface should be installed in the center of the tank for maximum effectiveness in reducing sloshing amplitude in practical engineering.

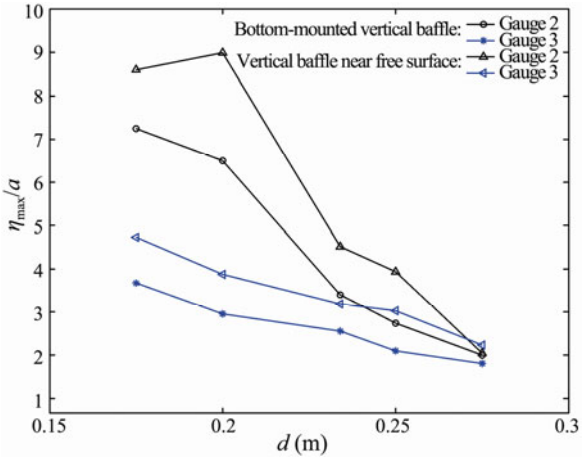


Fig.14 Maximum free surface elevation at wave gauges 2 and 3 in the first 25 s response to the distance of the vertical baffle from the left boundary of the tank for sloshing with the bottom-mounted vertical baffle and the vertical baffle touching the free surface when $x=-a\cos\omega t$, $a=0.03$ m, $h=0.2$ m, $\omega=\omega_0$, $d=0.275$ m, $h_b=0.15$ m.

Effects of the height of the vertical baffle touching the free surface on the free surface elevation are studied nu-

merically. The other parameters are the same except the height of the vertical baffle touching the free surface. The top of the vertical baffle touching the free surface with a different height is always the same height as the static free surface. Fig.15 presents comparisons of the time histories of the free surface elevation at wave Gauges 2 and 3 for the vertical baffle touching the free surface with $d$= 0.275 m and different height: (a) $h_b$=0.15 m, (b) $h_b$=0.12 m, (c) $h_b$=0.08 m, (d) $h_b$=0.05 m. The sloshing amplitude decreases with the increasing height of the vertical baffle touching the free surface. The wave amplitude attenuations of 86.7%, 82.5%, 78.5%, and 34.4% for Figs.15(a), 15(b), 15(c), and 15(d), respectively, are estimated according to Eq. (4). The ratio of the vertical baffle height to the water depth is defined as $\xi = h_b/h$, and the corresponding value of $\xi$ is 0.75, 0.6, 0.4, and 0.25 for Figs.15(a), 15(b), 15(c), and 15(d), respectively. The wave amplitude attenuation caused by the vertical baffle touching the free surface with a different height increases slowly with increasing vertical baffle height when the parameter $\xi$ is greater than 0.4.

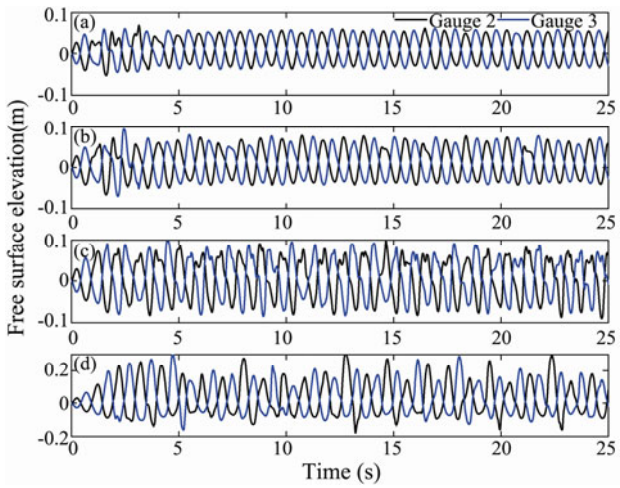


Fig.15 Comparisons of the time histories of the free surface elevation at wave gauges 2 and 3 for the vertical baffle touching the free surface with $d$=0.275 m and different $h_b$: (a) $h_b$=0.15 m, (b) $h_b$=0.12 m, (c) $h_b$=0.08 m, (d) $h_b$= 0.05 m.

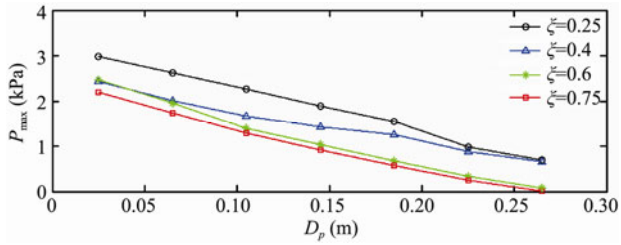


Fig.16 Maximum pressure distribution on the right tank wall for sloshing with different ratios of the vertical baffle height to water depth $\xi$, when excitation $\omega=\omega_0$.

Fig.16 shows the maximum pressure distribution on the right tank wall for sloshing with the vertical baffle touching the free surface with a different height. The $D_p$ and $P_{max}$ in Fig.16 are the distance of pressure measurement point to the bottom of the tank and the maximum impact pressure, respectively. Fig.16 shows that the maximum pressure that acts on the right tank wall decreases with the increasing ratio of the vertical baffle height to water depth $\xi$.

Effects of the excitation frequency on the free surface elevation and pressure are studied numerically and experimentally. The maximum free surface elevation at wave gauges 2 and 3 as a function of the excitation frequency with $h_b$=0.15 m, $x=-a\cos\omega t$, $a$=0.03 m, $h_b$= 0.2 m, $\omega_0$=6.5823 rad s$^{-1}$, and $d$=0.275 m is presented in Fig.17. The numerical results are in fairly good agreement with the experimental data in frequency domains ranging from 0.6$\omega_0$ to 1.1$\omega_0$, and the maximum free surface elevation at wave gauges 2 and 3 increase monotonically with increasing excitation frequency when $\omega/\omega_0\leq1$. This finding indicates that the first-mode natural frequency of the tank with the vertical baffle touching the free surface is greater than that of the tank without baffle, which is different from the law of sloshing with the bottom-mounted vertical baffle response to the excitation frequencies, as shown in Fig.8. The main reason is that the influence of the vertical baffle near the free surface on the natural frequency of the tank is more than the bottom-mounted vertical baffle, which make the first-mode natural frequency disappear. Moreover, it is commonly known that the horizontal velocity amplitude increases along with the central line from the tank bottom to the free surface. The blocking effect of the vertical baffle touching the free surface is thus more than the bottom-mounted vertical baffle.

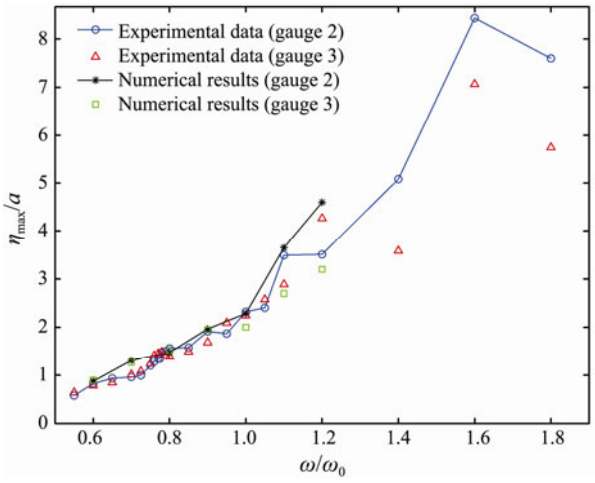


Fig.17 Maximum free surface elevation at wave gauges 2 and 3 response to the excitation frequency with $h_b$=0.15 m, $x=-a\cos\omega t$, $a$=0.03 m, $h$=0.2 m, $\omega_0$=6.5823 rad s$^{-1}$, $d$=0.275 m.

Fig.18 displays the maximum pressure at sensors P1, P2, and P3 response to the excitation frequencies when the vertical baffle with $h_b$=0.15 m was installed near the free surface. The locations of three pressure sensors are presented in Fig.11. The numerical results of pressure at the three pressure sensors are also in good agreement with the present experimental data. Fig.18 shows that the maximum pressure at sensors P1, P2, and P3 also in-

creases with increasing external excitation frequency when $\omega/\omega_0 \leq 1$.

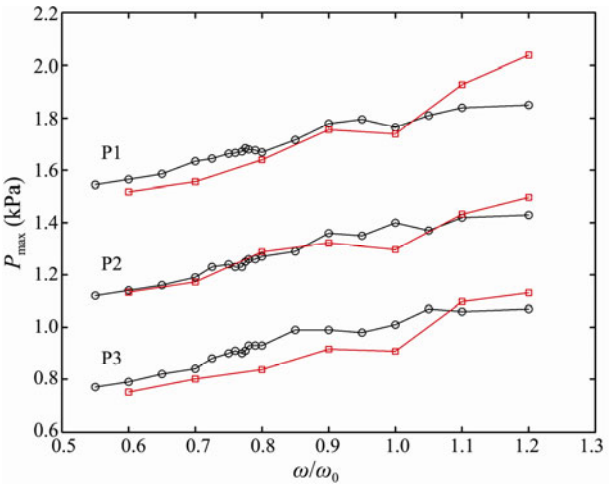


Fig.18 Maximum pressure at pressure sensors P1, P2, and P3 response to the excitation frequency when $h_b=0.15$ m, $x=-a\cos\omega t$, $a=0.03$ m, $h=0.2$ m, $\omega_0=6.5823$ rad s$^{-1}$, $d=0.275$ m. (—○— Experimental data, —□— Numerical results).

### 4.3 Comparisons of Pressure for Sloshing with Two Types of Vertical Baffle

Predicting sloshing pressure distribution is important to optimizing the design of liquid tanks. Despite previous theoretical and numerical efforts to predict sloshing pressure, the physical model experiment is still considered the most reliable method for practical purposes. In this section, effects of the location of the bottom-mounted vertical baffle and the vertical baffle touching the free surface on pressure distribution at three pressure sensors equipped on the right tank wall are presented. Fig.19 shows comparisons of the maximum impact pressure on the right tank wall response to the distance of the vertical baffle from the left boundary of the tank for sloshing with the bottom-mounted vertical baffle and the vertical baffle touching the free surface when $x=-a\cos\omega t$, $a=0.03$ m, $\omega=\omega_0$, $h=0.2$ m, and $h_b=0.15$ m. Fig.19 shows that the maximum impact pressure at P1, P2, and P3 decreases with the increasing distance of the vertical baffle touching the free surface from the left boundary of the tank and is slightly greater than that of sloshing with the bottom-mounted vertical baffle aside from the case where the vertical baffle located at the center of the tank. This finding indicates that the bottom-mounted vertical baffle more effectively reduces sloshing impact pressure than the vertical baffle touching the free surface when the vertical baffle deviates from the tank center. For sloshing with the bottom-mounted vertical baffle, Fig. 16 shows that the effects of the vertical baffle location on impact pressure distribution near the tank bottom, such as P1 and P2, are not remarkable.

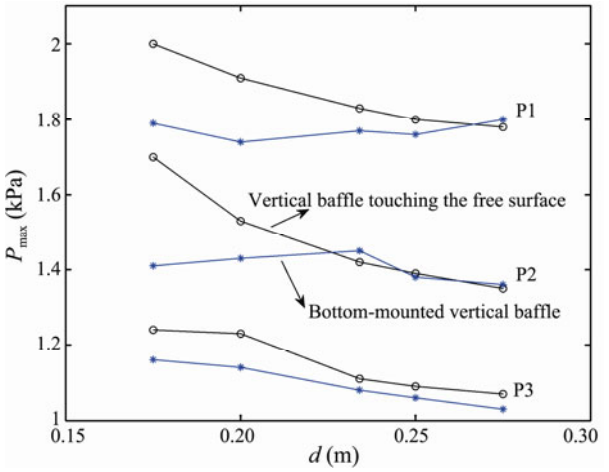


Fig.19 Comparisons of the maximum pressure on the right tank wall response to the distance of the vertical baffle from the left boundary of the tank for sloshing with the bottom-mounted vertical baffle and the vertical baffle touching the free surface when $x=-a\cos\omega t$, $a=0.03$ m, $\omega=\omega_0$, $h=0.2$ m, and $h_b=0.15$ m.

The vertical baffle located at the tank center is generally considered the most effective in reducing sloshing. Fig.20 plots comparisons of the maximum impact pressure on the right tank wall as a function of the excitation frequencies for sloshing with both the bottom-mounted vertical baffle and the vertical baffle touching the free surface with $x=-a\cos\omega t$, $a=0.03$ m, $h=0.2$ m, $d=0.275$ m, and $h_b=0.15$ m is plotted in Fig.20. The maximum impact pressure at P1, P2, and P3 of sloshing with the bottom-mounted vertical baffle is greater than that of sloshing with the vertical baffle touching the free surface in the frequencies ranging from $0.55\omega_0$ to $0.9\omega_0$ and roughly equivalent in other frequencies. This finding indicates that the vertical baffle touching the free surface is more effective than the bottom-mounted vertical baffle in reducing the sloshing pressure. Moreover, the maximum impact pressure at P1, P2, and P3 of sloshing with the bottom-mounted vertical baffle increases first to a peak at around $0.77\omega_0$ and then decreases with the increase in the external excitation frequency before the frequency $0.88\omega_0$ and then increases roughly when the frequency increases from $0.88\omega_0$ to $1.2\omega_0$. However, the maximum impact pressure at three pressure sensors of sloshing with the vertical baffle touching the free surface increases roughly with increasing external excitation frequency, thereby indicating that no resonant sloshing phenomenon occurs in the frequencies ranging from $0.55\omega_0$ to $1.2\omega_0$. This behavior is in agreement with the results of the maximum free surface elevation response to the external excitation frequency.

The time histories of the dynamic pressure at P3 for the sloshing in tanks without baffle, with the bottom-mounted vertical baffle, and with the vertical baffle touching the free surface is plotted in Fig.21. The dynamic pressure amplitude at P3 is reduced to the minimum level by introducing the vertical baffle, especially the vertical baffle touching the free surface when the excitation frequency is equal to the first-mode natural frequency without the baffle. This finding indicates that the vertical baffle touching the free surface is more effective than the bottom- mounted vertical baffle in reducing the sloshing-induced dynamic pressure distribution. Moreover, the dynamic pressure amplitude under the resonant frequency is far greater than

that with the excitation frequency of $\omega=0.77\omega_0$. In addition, double peaks of the time history of the dynamic pressure are remarkably observed in sloshing without baffle and with the bottom-mounted vertical baffle. However, these peaks disappear in sloshing with the vertical baffle touching the free surface when the excitation frequency is$\omega=0.77\omega_0$.

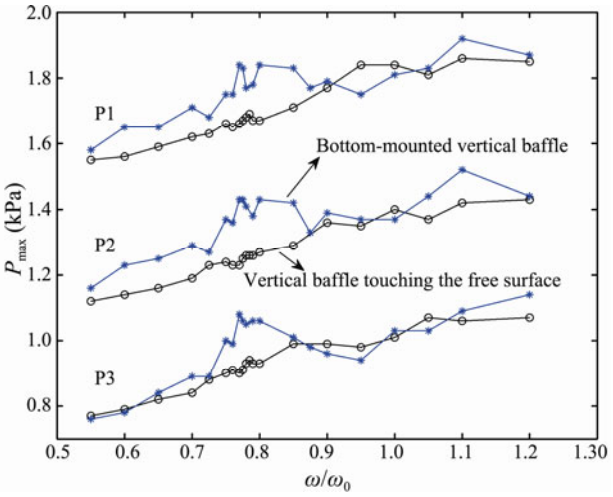


Fig.20 Comparisons of the maximum pressure on the right tank wall response to the excitation frequencies for sloshing with the bottom-mounted vertical baffle and the vertical baffle touching the free surface when $x=-a\cos\omega t$, $a=0.03$ m, $h=0.2$ m, $d=0.275$ m, and $h_b=0.15$ m.

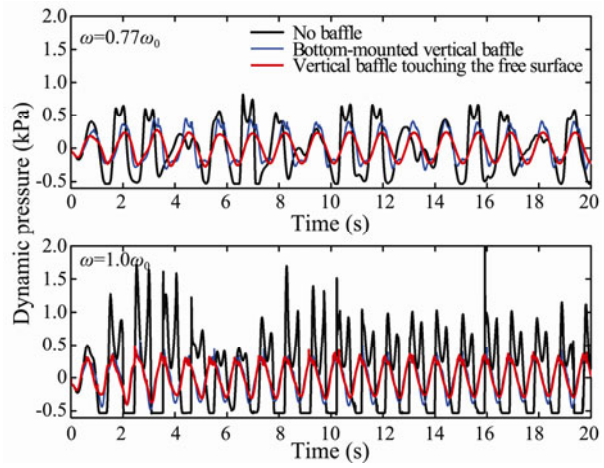


Fig.21 Comparisons of the time histories of the dynamic pressure at P3 among the sloshing in tanks without baffle, with the bottom-mounted vertical baffle, and with the vertical baffle touching the free surface for $x=-a\cos\omega t$, $a=0.03$ m, $h=0.2$ m, $d=0.275$ m, and $h_b=0.15$ m.

To depict and compare the violent sloshing process in the rectangular tank without a baffle, with the bottom-mounted vertical baffle, and with the vertical baffle touching the free surface, sloshing snapshots at $t=2.25$ s, 2.80 s, 3.35 s, 3.90 s are shown in Fig.22. The sloshing waves without the baffle climb the highest, and wave breaking occurs subsequently. Fig.22 also shows that the liquid mass involved in sloshing without the baffle is also far greater than that with the vertical baffle. As shown in Fig.21, the slamming pressure on the tank wall is the greatest. For sloshing with the bottom-mounted vertical baffle, numerous air bubbles are trapped in the fluids on both sides of the vertical baffle. Fig.22 shows that the sloshing waves generally break near the tank walls in sloshing without the baffle on both sides of the vertical baffle for sloshing with the vertical baffle. The sloshing-induced slamming pressure on the tank walls is therefore reduced by the vertical baffle.

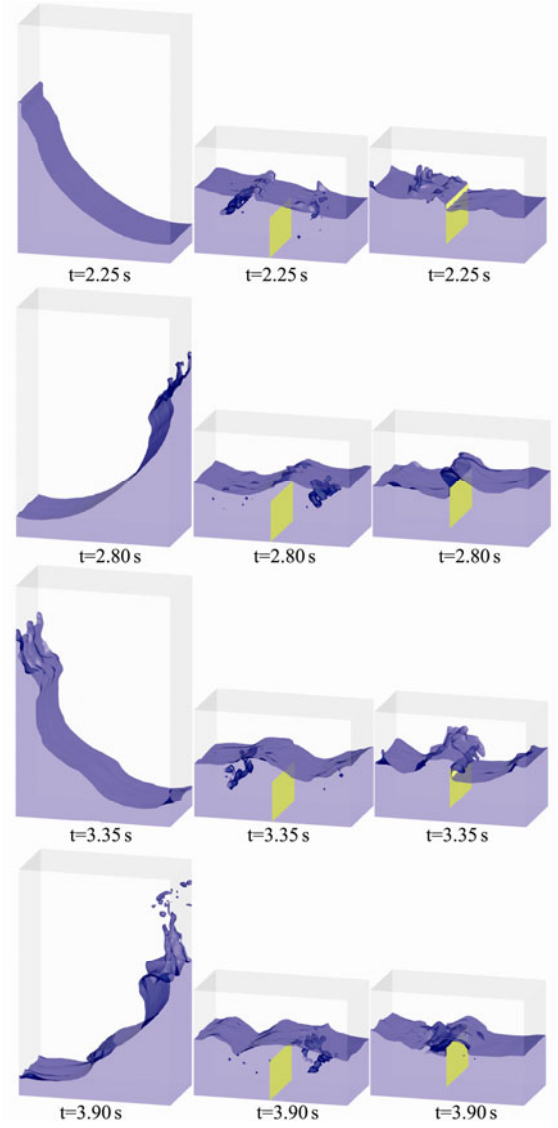


Fig.22 Snapshots of sloshing in a rectangular tank without baffle, with the bottom-mounted vertical baffle, and with the vertical baffle touching the free surface for $x=-a\cos\omega t$, $a=0.03$ m, $\omega=\omega_0$, $h=0.2$ m, $d=0.275$ m, and $h_b=0.15$ m.

## 5 Conclusions

In this study, a finite difference turbulence model is used to simulate sloshing problems in rectangular tank with different types of vertical baffle. Laboratory experiments are conducted to confirm the validity of the proposed numerical model. Good agreement is observed between the present numerical results and the current experimental data.

For the sloshing with the bottom-mounted vertical baf-

fle and the vertical baffle touching the free surface, the sloshing amplitude decreases gradually when the vertical baffle is moved to the center of the tank, and it decreases with increasing height of the vertical baffle when it is located at the center of the tank. In addition, the maximum sloshing amplitude and pressure on the right tank wall of the sloshing with the vertical baffle touching the free surface is always greater than that of the sloshing with the bottom-mounted vertical baffle when the vertical baffle is not located at the center of the tank. However, the first-mode natural frequency of the baffled tank shifts to a lower frequency for the sloshing with the bottom-mounted vertical baffle, and it shifts to a higher frequency for the sloshing with the vertical baffle touching the free surface compared with the unbaffled tank when the vertical baffle is located at the center of the tank. The maximum impact pressure on the right tank wall of the sloshing with the bottom-mounted vertical baffle is greater than that of the sloshing with the vertical baffle touching the free surface in the frequencies ranging from $0.55\omega_0$ to $0.88\omega_0$, and it is roughly equivalent in the frequencies $0.88\omega_0$ to $1.2\omega_0$ when the vertical baffle is located at the center of the tank.

The vertical baffle touching the free surface and located at the center of the tank is more effective than the bottom-mounted vertical baffle in reducing sloshing amplitude and pressure. The main reason is that the maximum horizontal velocity component is at the center of the tank, and its amplitude increases along with the central line from the tank bottom to the free surface. Therefore, the blocking effect and influence of the vertical baffle touching the free surface on the natural frequency of the tank is more than the bottom-mounted vertical baffle. Besides, the sharp edges length of the vertical baffle touching the free surface is larger than the bottom-mounted vertical baffle, thus more vortices were generated near the sharp edges and more energy dissipation occurred in small-scale vortices. To demonstrate these findings, images of the sloshing in the baffled tank and unbaffled tank are shown.

## Acknowledgement

This study is supported by the National Natural Science Foundation of China (Nos. 51679079 and 51209080), the Fundamental Research Funds for the Central Universities (No. 2014B17314), the Program for Excellent Innovative Talents of Hohai University, the Open Fund of State Key Laboratory of Hydraulic Engineering Simulation and Safety, Tianjin University (HESS-1703), the Open Fund Program of Key Laboratory of Water & Sediment Science and Water Hazard Prevention, Changsha University of Science & Technology (2015SS03), and the 111 Project (B12032).

## References

Akyildiz, H., 2012. A numerical study of the effects of the vertical baffle on liquid sloshing in two-dimensional rectangular tank. *Journal of Sound and Vibration*, **331**: 41-52.

Buzhinskii, V. A., 1998. Vortex damping of sloshing in tanks with baffles. *Journal of Applied Mathematics and Mechanics*, **62** (2): 217-224.

Cho, J. R., Lee, H. W., and Kim, K. W., 2002. Free vibration analysis of baffled liquid-storage tanks by the structural-acoustic finite element formulation. *Journal of Sound and Vibration*, **258**: 847-866.

Faltinsen, O. M., and Timokha, A. N., 2009. *Sloshing*. Cambridge University Press, New York, 577pp.

Gandhi, P. S., Joshi, K. B., and Ananthkrishnan, N., 2008. Design and development of a novel 2DOF actuation slosh rig. *Journal of Dynamic Systems, Measurement, and Control*, **131** (1): 011006.

Gedikli, A., and Erguven, M. E., 1999. Seismic analysis of a liquid storage tank with a baffle. *Journal of Sound and Vibration*, **223**: 141-155.

Ibrahim, R. A., 2005. *Liquid Sloshing Dynamics: Theory and Applications*. Cambridge University Press, New York, 970pp.

Kim, H. S., and Lee, Y. S., 2008. Optimization design technique for reduction of sloshing by evolutionary methods. *Journal of Mechanical Science and Technology*, **22** (1): 25-33.

Liu, D. M., and Lin, P. Z., 2008. A numerical study of three-dimensional liquid sloshing in tanks. *Journal of Computational Physics*, **227**: 3921-3939.

Liu, D. M., and Lin, P. Z., 2009. Three-dimensional liquid sloshing in a tank with baffles. *Ocean Engineering*, **36**: 202-212.

Lu, L., Jiang, S. C., Zhao, M., and Tang, G. Q., 2015. Two-dimensional viscous numerical simulation of liquid sloshing in rectangular tank with/without baffles and comparison with potential flow solutions. *Ocean Engineering*, **108**: 662-677.

Qin, J. M., Chen, B., and Lu, L., 2013. Finite element based viscous numerical wave flume. *Advances in Mechanical Engineering*, **2013**: 1-17.

Rebouillat, S., and Liksonov, D., 2010. Fluid-structure interaction in partially filled liquid containers: A comparative review of numerical approaches. *Computers & Fluids*, **39** (5): 739-746.

Shin, J. R., Choi, K. S., and Kang, S. Y., 2005. An analytical solution to sloshing natural periods for a prismatic liquid cargo tank with baffles. *Journal of Ocean Engineering and Technology*, **19**: 16-21.

Tuner, M. R., Bridges, T. J., and Ardakani, H. A., 2013. Dynamic coupling in Cooker's sloshing experiment with baffles. *Physics of Fluids*, **25 (11)**: 385-395.

Xue, M. A., and Lin, P. Z., 2011. Numerical study of ring baffle effects on reducing violent liquid sloshing. *Computers & Fluids*, **52**: 116-129.

Xue, M. A., Lin, P. Z., Zheng, J. H., Ma, Y. X., Yuan, X. L., and Nguyen, V. T., 2013. Effects of perforated baffle on reducing sloshing in rectangular tank: Experimental and numerical study. *China Ocean Engineering*, **27** (5): 615-628.

Xue, M. A., Zheng, J. H., Lin, P. Z., and Yuan, X. L., 2017. Experimental study on vertical baffles of different configurations in suppressing sloshing pressure. *Ocean Engineering*, **136**: 178-189.

Younes, M. F., Younes, Y. K., El-Madah, M., Ibrahim, I. M., and El-Dannanh, E. H., 2007. An experimental investigation of hydrodynamic damping due to vertical baffle arrangements in a rectangular tank. *Proceedings of the Institution of Mechanical Engineers, Part M: Journal of Engineering for the Maritime Environment*, **221** (3): 115-123.

**(Edited by Xie Jun)**